Hybrid 18F-labeled Fluoride Positron Emission Tomography / Magnetic Resonance (MR) Imaging of the Sacroiliac Joints and the Spine in Patients with Axial Spondyloarthritis: A Pilot Study Exploring the Link of MR Bone Pathologies and Increased Osteoblastic Activity

Christian Buchbender, Benedikt Ostendorf, Verena Ruhlmann, Philipp Heusch, Falk Miese, Karsten Beiderwellen, Matthias Schneider, Juergen Braun, Gerald Antoch, and Xenofon Baraliakos

ABSTRACT. ***Objective.*** The biologically active molecule used in positron emission tomography (PET) for depiction of osteoblastic activity is 18F-labeled fluoride (18F-F). We examined whether inflammatory or chronic changes on magnetic resonance imaging (MRI) in the sacroiliac joints (SIJ) and the spines of patients with active ankylosing spondylitis (AS) are linked to osteoblastic activity, assessed by PET/MRI.

Methods. Thirteen patients with AS (mean age 37.8 ± 11.4 yrs, Bath AS Disease Activity Index > 4, no anti-TNF treatment) underwent 3-Tesla whole-spine and SIJ PET/MRI. Two independent readers recorded pathologic changes related to vertebral (VQ) or SIJ quadrants (SQ). Final scores were based on reader agreement.

Results. A total of 104 SQ and 1196 VQ were examined. In SIJ, bone marrow edema (BME) was seen in 44.2%, fat deposition (FD) in 42.3%, and 18F-F in 46.2% SQ. BME alone was associated with 18F-F in 78.6% and FD alone in only 7.7% SQ, while the combination BME/FD was associated with 18F-F in 72.2% SQ. Erosions, sclerosis, and ankylosis alone were rarely associated with 18F-F. In the spine, BME alone was seen in 9.9%, FD in 18.2%, and 18F-F in 5.4% VQ. BME alone was associated with 18F-F in 14.3% and FD alone in 8.7% VQ, while the combination BME/FD was associated with 18F-F in 40.6% VQ.

Conclusion. In this study of hybrid 18F-F PET/MRI of patients with active AS, we show that BME rather than chronic changes is associated with osteoblastic activity, while the combination of BME and FD showed the highest 18F-F uptake. The use of PET/MRI in prediction of future syndesmophyte formation in AS needs further exploration in prospective studies. (First Release July 1 2015; J Rheumatol 2015;42:1631–7; doi:10.3899/jrheum.150250)

Key Indexing Terms:
AXIAL SPONDYLOARTHRITIS
ANKYLOSING SPONDYLITIS
SPONDYLOARTHRITIDES
PET/MRI
MR-PET

Ankylosing spondylitis (AS) is 1 main entity of the axial spondyloarthritides (axSpA) and represents a frequent autoimmune-mediated chronic inflammatory disease that predominantly affects the spine and the sacroiliac joints (SIJ)[1]. Driven by inflammation, progressive stiffness and postural deformation in the axial skeleton of patients with AS results in severe functional disability[1]. Antiinflammatory compounds such as nonsteroidal antiinflammatory drugs (NSAID) or biologic agents, such as antibodies inhibiting tumor necrosis factor-α (TNF-α), are used to treat patients

From the Department of Diagnostic and Interventional Radiology, and Department of Rheumatology, Medical Faculty, University of Dusseldorf, Dusseldorf; Department of Nuclear Medicine, and Department of Diagnostic and Interventional Radiology and Neuroradiology, Medical Faculty, University of Duisburg-Essen, Essen; Rheumazentrum Ruhrgebiet Herne, Ruhr-University Bochum, Herne, Germany.

C. Buchbender, MD, Department of Diagnostic and Interventional Radiology; B. Ostendorf, MD, Department of Rheumatology, Medical Faculty, University of Dusseldorf; V. Ruhlmann, MD, Department of Nuclear Medicine, Medical Faculty, University of Duisburg-Essen; P. Heusch, MD; F. Miese, MD, Department of Diagnostic and Interventional Radiology, Medical Faculty, University of Dusseldorf; K. Beiderwellen, MD, Department of Diagnostic and Interventional Radiology and Neuroradiology, Medical Faculty, University of Duisburg-Essen; M. Schneider, MD, Department of Rheumatology, Medical Faculty, University of Dusseldorf; J. Braun, MD, Rheumazentrum Ruhrgebiet Herne, Ruhr-University Bochum; G. Antoch, MD, Department of Diagnostic and Interventional Radiology, Medical Faculty, University of Dusseldorf; X. Baraliakos, MD, Rheumazentrum Ruhrgebiet Herne, Ruhr-University Bochum.

Address correspondence to Dr. X. Baraliakos, Rheumazentrum Ruhrgebiet Herne, Ruhr-University Bochum, Claudiusstr. 45, 44649 Herne, Germany. E-mail: baraliakos@me.com

Accepted for publication May 6, 2015.

with axSpA, depending on their disease activity status[2,3]. Imaging of the axial skeleton and the SIJ is important for classification to axSpA and the final diagnosis, and it is also used for the prediction and assessment of response to treatment[4]. Historically, conventional radiography is the imaging gold standard in AS because it reliably depicts the formation of new bone, such as SIJ ankylosis or syndesmophytes[5]. However, because these radiographic features reflect structural changes of established disease, imaging modalities that are able to depict early stages (characterized by inflammation) have been developed.

In this context, magnetic resonance imaging (MRI) has been increasingly used for imaging of the spine and the SIJ in AS. Inflammatory MRI lesions have been shown to be related to structural changes[6] and MRI has been demonstrated to be sensitive to changes under antiinflammatory therapy in numerous studies[7]. In a recent trial that examined the relationship of spinal inflammation [assessed by bone marrow edema (BME)] and postinflammatory changes [assessed by fat deposition (FD)] as detected by MRI, and new bone formation (assessed by the occurrence of syndesmophytes) as detected by conventional radiographs in patients with active AS[8], we could show that either the inflammatory activity that later developed to FD or the parallel occurrence of inflammation and fatty degeneration prior to treatment were significantly associated with syndesmophyte formation after 5 years of anti-TNF therapy.

The ongoing trend of the identification of molecular therapeutic targets in rheumatic diseases also induced changes to the field of diagnostic imaging — away from the mere depiction of structural changes to the visualization of pathologic molecular tissue characteristics. In this context, the diagnostic potential of nuclear imaging with single-photon emission tomography and positron emission tomography (PET) have also been investigated[9]. This evolution led to the development of so-called hybrid imaging modalities, integrated PET and MRI (PET/MRI). The simultaneous acquisition of high-resolution anatomical and functional magnetic resonance (MR) images and metabolic information known to be possible by PET is expected to provide new insights into the link between inflammatory cascades, local metabolic changes, and the development of structural manifest inflammation. PET/computed tomography (CT) studies in AS with 18F-labeled fluoride (18F-F), a tracer that depicts specifically osteoblastic activity[10], revealed that increased tracer uptake is only modestly correlated to BME on MRI, but may be mainly correlated to structural changes[11,12]. However, to date, there are no data available on the use of true hybrid whole-spine 18F-F PET/MRI in AS.

The aim of our pilot study was to examine the relationship between inflammatory and postinflammatory changes as assessed by MRI of the SIJ and the spine of patients with active AS and the visualization of local osteoblastic activity as assessed by focal 18F-F uptake in PET/MRI.

MATERIALS AND METHODS

Patients. After review board approval (University of Duisburg-Essen, Germany), patients were consecutively recruited after giving informed consent. All patients had to have the diagnosis of established AS according to the modified New York criteria[13], be in a status of active disease (Bath AS Activity Index[14] > 4 out of 10 units), and have not been treated with an anti-TNF compound. Other medication, such as NSAID, was not discontinued prior to the imaging examinations. A total of 13 patients [6 men, 7 women, mean age (± SD) 37.8 (± 11.4)] were included in our PET/MRI study.

Imaging. PET/MRI was performed on a Magnetom Biograph mMR (Siemens Healthcare) that consisted of a 3T-MRI scanner. The scan was performed in the mineralization phase 40 min after injection of a mean dose 157 MBq of 18F-F and was performed in caudocranial direction, starting with the SIJ. The field of view (FoV) contained the whole spinal axis from the atlas to the coccyx. PET acquisition time was 5 min per bed position. PET images were reconstructed using the iterative algorithm ordered subset expectation maximization, 3 iterations, and 21 subsets, Gaussian filter: full width at half maximum 4.0 mm, scatter correction. Beside the built-in body coil, a dedicated mMR neck coil was used for MR imaging. MR imaging was performed simultaneously to PET imaging using the following sequence protocol per bed position:

(1) A coronal 3-D volumetric interpolated breath-hold examination (VIBE) sequence [repetition time (TR) 3.6 ms, echo time 1 (TE) 1.23 ms, TE2 2.46 ms, 3.12 mm slice thickness, FoV 500 mm] for Dixon-MRI–based PET attenuation and scatter correction.

(2) A sagittal (coronal for SIJ) 2-dimensional T2-weighted turbo spin echo sequence [TR 4000 ms, TE 107 ms, matrix size 256, 3 mm slices, FoV 280 mm, generalized auto calibrating partially parallel acquisition (Group for Research and Assessment of Psoriasis and Psoriatic Arthritis; GRAPPA), acceleration factor 2].

(3) A sagittal (coronal for SIJ) 2-dimensional T2-weighted turbo inversion recovery sequence with magnitude (TIRM) with fat suppression (TR 3780 ms, TE 58 ms, inversion time 220 ms, matrix size 256, 3 mm slice thickness, FoV 280 mm, GRAPPA, acceleration factor 2).

(4) A sagittal (coronal for SIJ) 2-dimensional T1-weighted TIRM with spinal fluid suppression (TR 2000 ms, TE 13 ms, inversion time 900 ms, matrix size 256, 3 mm slice thickness, FoV 280 mm, GRAPPA, acceleration factor 2).

PET/MRI image fusion was performed for all sequences, except for the VIBE images, which were solely used for PET calibration.

Image analysis and scoring. All MR and PET images were read by 2 experienced readers independently in random patient order and blinded for patients' demographics. MR images and PET images were read in separate sessions so that the reader would not be influenced by findings at the corresponding sites by looking at both imaging modalities simultaneously. For the final analysis, only lesions where both readers reported agreement were taken into account. In the analysis of the spine, inflammatory activity (BME) on TIRM, FD on T1, and focal 18F-F uptake were recorded on the level of a vertebral quadrant (VQ), where 1 vertebral body consisted by 4 VQ (superior anterior and posterior, and inferior anterior and posterior). In the analysis of the SIJ, the iliac and sacral parts of the SIJ were each subdivided into an upper (including the first sacral foramen) and a lower part (including the second and third sacral foramina), resulting in 4 SIJ quadrants (SQ) per side. SQ were scored separately for the presence of BME on TIRM, FD, erosions, sclerosis, and ankylosis on T1 and focal 18F-F uptake, respectively. For the semiquantitative analysis, the maximum standardized uptake values (SUVmax; no specific units provided) in 18F-F PET images were measured by an independent radiologist in those lesions where both blinded readers reported agreement and by using a volume of interest covering the entire individual lesion.

Statistical analysis. Descriptive statistics (mean values ± SD) were used for demographic data, PET/MRI findings, and SUVmax. Proportions of VQ and SQ showing BME, FD, syndesmophyte formation, erosions, sclerosis,

increased 18F-F uptake, or any combination of these findings were calculated to investigate the coincidence of inflammatory PET and MRI changes. Similar to previous reports[15] and because of the low patient numbers included in this pilot study, reliability between readers was performed in a descriptive way. The number of lesions seen by both readers or by only 1 of the 2 readers was assessed, and the latter cases were discussed by consensus-reading in a joint session of both readers. In case both readers agreed about the occurrence of a positive signal, these lesions were also taken into account for the final analyses.

RESULTS

Acquisition of whole-spine 18F-F PET/MRI including the SIJ was successful in all patients. Diagnostic image quality of PET and MRI and precision of image coregistration was high (Figure 1, Figure 2, and Figure 3. There was excellent agreement in the reading of the 2 readers, with 96% of all lesions reported being seen by both readers and only 4% needing a consensus reading, in which agreement was seen in all cases.

Relationship between focal 18F-F uptake and MRI pathologies. In the SIJ, a total of 104 SQ could be analyzed by MRI and PET/MRI. Out of those, 46 SQ (44.2%) showed BME (Figure 1A, Figure 2A), while FD (Figure 1B, Figure 2B) was found in 44 SQ (42.3%) and focal 18F-F uptake in 48 SQ (46.2%; Figure 1C, Figure 2C). BME without concomitant FD was found in 28/46 SQ (60.9%), and in those, parallel occurrence of focal 18F-F uptake was seen in 22 SQ (78.6%). In comparison, FD alone without concomitant BME (Figure 1B) was found in 26/44 SQ (59.1%), and in those, parallel occurrence of focal 18F-F uptake was seen in only 2 SQ (7.7%). The difference in the same pattern of SQ with BME (Figure 2B) was statistically significant (Table 1). Finally the combination of BME and FD was found in 18 SQ and in those, parallel occurrence of focal 18F-F uptake (Figure 2A–C) was seen in 13 SQ (72.2%). The difference to the VQ with FD without BME but with focal 18F-F uptake was statistically significant (Table 1).

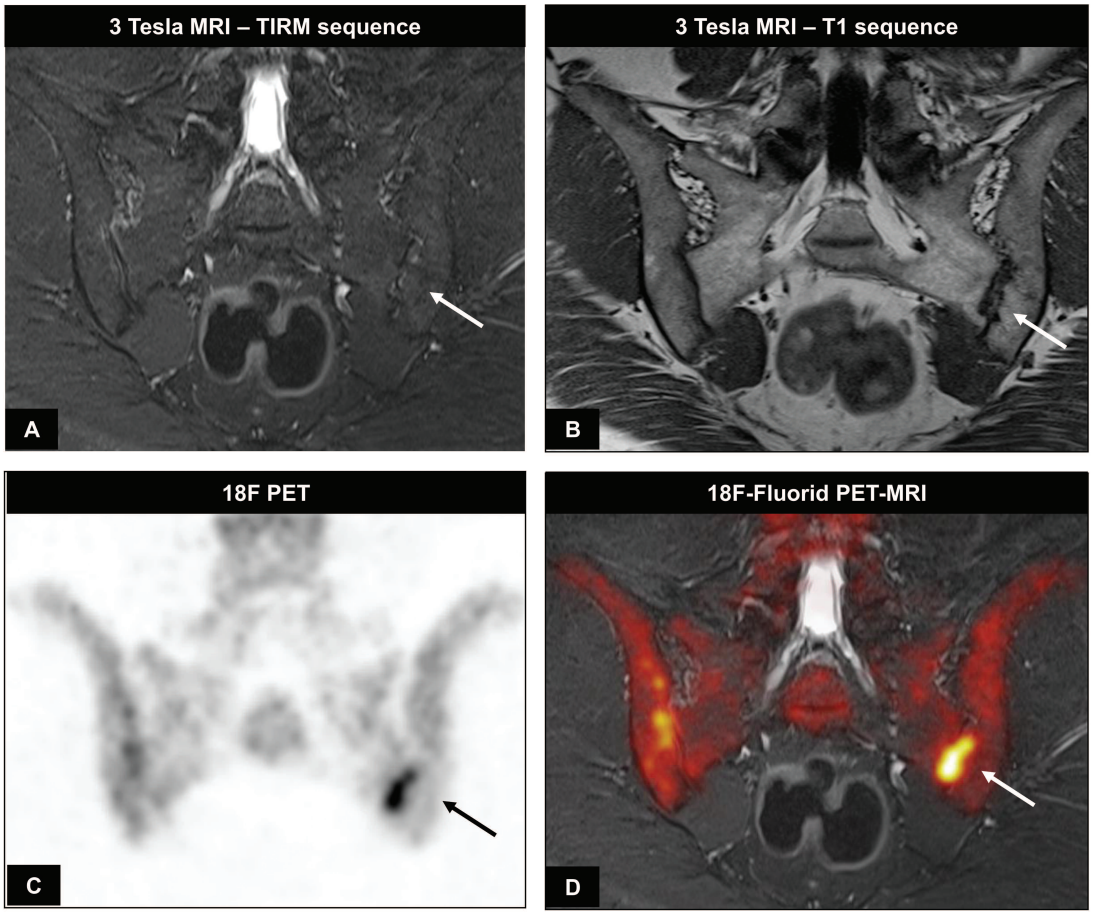

Figure 1. SIJ of a 36-year-old patient with active AS. A. 3 Tesla MRI in TIRM sequence. B. 3 Tesla MRI in T1 sequence. C. 18F-F PET. D. 18F-F PET/MRI. Increased signal in the 18F-F PET and PET/MRI indicates an area without BME activity, but with high metabolic activity that is characterized by fat degeneration and erosions (as seen on the T1 sequence; panel B). AS: ankylosing spondylitis; MRI: magnetic resonance imaging; TIRM: turbo inversion recovery sequence with magnitude; 18F-F: 18F-labeled fluoride; PET: positron emission tomography; SIJ: sacroiliac joints; BME: bone marrow edema.

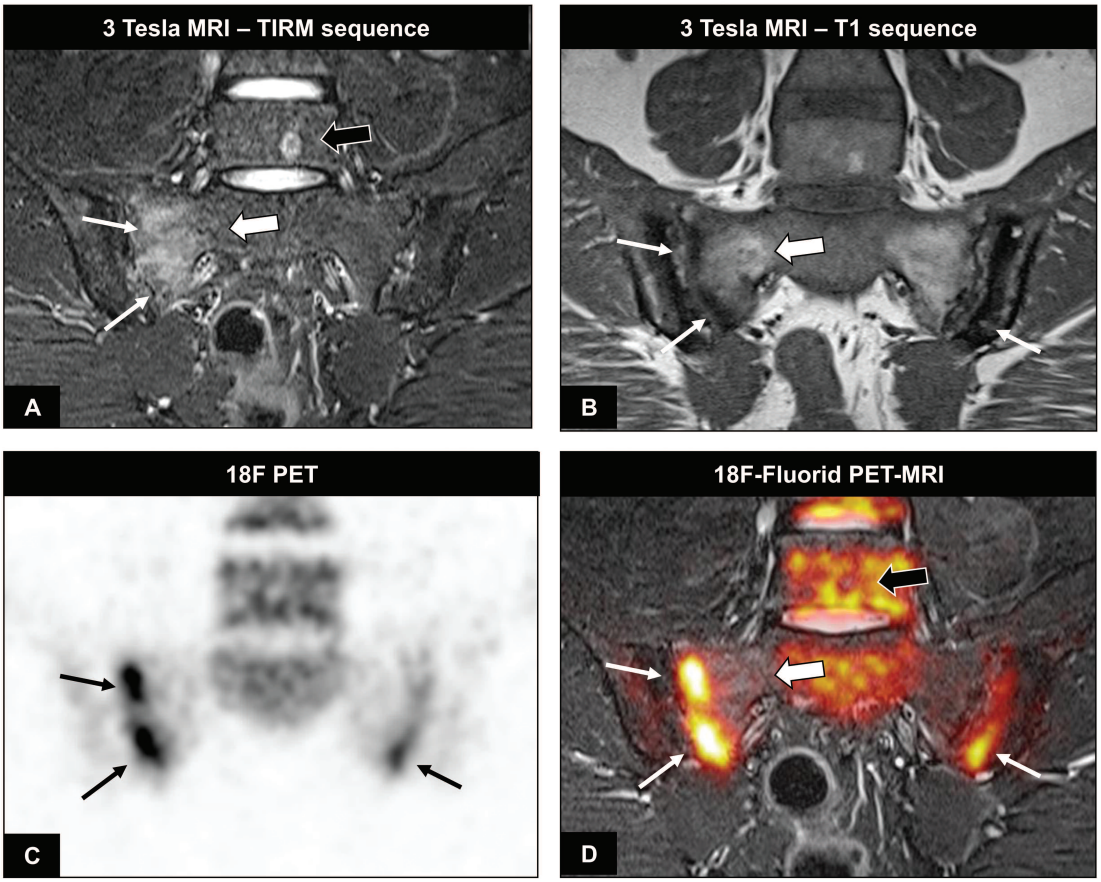

Figure 2. SIJ of a 28-year-old patient with active AS. A. 3 Tesla MRI in TIRM sequence. B. 3 Tesla MRI in T1 sequence. C. 18F-F PET. D. 18F-F PET/MRI. Increased signal in the 18F-F PET/MRI of the right SIJ indicates an area with periarticular sclerosis and erosions (white thin arrows) surrounded by BME and fatty degeneration (white thick arrows). In the left inferior iliac region, activity on PET corresponds to an area of erosion and sclerosis without either BME or fatty changes. As a signal of specificity to increased fluoride metabolism because of AS, but not because of any other reason in the TIRM MRI, the hemangioma in the fifth lumbar vertebra (black thick arrow) is visible on TIRM MRI but not in the 18F-F PET/MRI. AS: ankylosing spondylitis; MRI: magnetic resonance imaging; TIRM: turbo inversion recovery sequence with magnitude; 18F-F: 18F-labeled fluoride; PET: positron emission tomography; SIJ: sacroiliac joints; BME: bone marrow edema.

Other lesions, such as erosions, sclerosis (Figure 1, Figure 2), or bony bridges, were not associated with focal 18F-F uptake unless they were accompanied by BME (Table 1).

Overall, focal 18F-F uptake without concomitant BME or FD was found in 11 SQ (10.6% of all evaluated SQ and 22.9% of the SQ with focal 18F-F uptake).

Spine. A total of 1196 VQ could be analyzed by MRI and PET/MRI. Out of those, 118 VQ (9.9%) showed BME (Figure 3A), while FD was found in 218 VQ (18.2%; Figure 3B) and focal 18F-F uptake in 65 VQ (5.4%; Figure 3C). BME without concomitant FD (Figure 3A) was found in 49/118 VQ (41.5%), and in those, parallel occurrence of focal 18F-F uptake was seen in 7 VQ (14.3%). In comparison, FD alone (Figure 3B) without concomitant BME was found in 149/218 VQ (68.3%), and in those, parallel occurrence of focal 18F-F uptake was seen in 13 VQ (8.7%; Figure 3C). Finally, the combination of BME and FD was found in 69 VQ, and in those, parallel occurrence of focal 18F-F uptake was seen in 28 VQ (40.6%). The difference in the VQ with BME without FD, but with focal 18F-F uptake, or in VQ with FD without BME, but with focal 18F-F uptake, was statistically significant (Table 1).

Overall, focal 18F-F uptake without concomitant BME or FD was found in 17 VQ (1.4% of all evaluated VQ and 26.2% of the VQ with focal 18F-F uptake).

Correlation of SUVmax in 18F-F PET/MRI to other imaging findings. In the SIJ, the highest mean SUVmax was found in SQ with a combination of BME and FD (28.1 ± 13.5), followed by SQ where focal 18F-F uptake was associated with FD, but no BME (27.3 ± 17.6), or SQ where focal 18F-F uptake was associated with BME, but no FD (21.8 ± 17.7, all p = not significant). Focal 18F-F uptake without association with any MRI lesions had a mean SUVmax of 16.5 ± 6.0.

Spine. SUVmax intensity in the spine was similar between

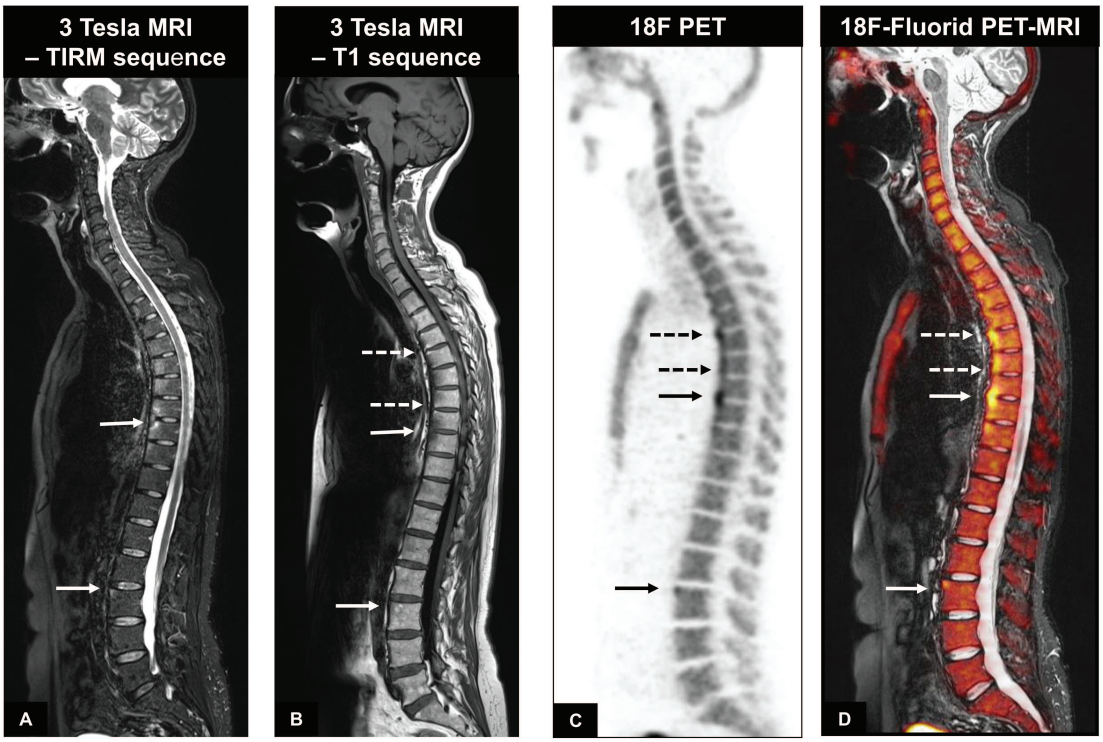

Figure 3. Spine of a 55-year-old patient with active AS. A. 3 Tesla MRI in TIRM sequence. B. 3 Tesla MRI in T1 sequence. C. 18F-F PET. D. 18F-F PET/MRI. In 18F-F PET/MRI, increased signal indicates metabolic processes that can be seen in areas with BME (complete arrows) and also in areas with FD (incomplete arrows). AS: ankylosing spondylitis; MRI: magnetic resonance imaging; TIRM: turbo inversion recovery sequence with magnitude; 18F-F: 18F-labeled fluoride; PET: positron emission tomography; BME: bone marrow edema; FD: fat deposition.

Table 1. Number and proportion of lesions on MRI and PET/MRI for the SIJ and the spine. Values are n (%) unless otherwise specified.

Lesions		BME	FD	p	BME + FD	p	PET	Erosions	Sclerosis	Ankylosis
SIJ	Total (%), n = 104	46 (44.2)	44 (42.3)	NS	18 (17.3)	—	48 (46.2)	34 (32.2)	20 (19.2)	10 (9.6)
	Total (%) + PET	35 (67.1)	15 (34.1)	< 0.001	13 (72.2)	NS*, 0.005**	—	21 (61.8)	11 (55)	0
	Sole total (%)	28 (60.9)	26 (59.1)	NS	—	—	11 (22.9)	6	4	0
	Sole total (%) + PET	22 (78.6)	2 (7.7)	< 0.001	—	—	—	1 (16.7)	2 (50)	0
Spine	Total (%), n = 1196	118 (9.9)	218 (18.2)	< 0.001	69 (9.9)	—	65 (5.4)	—	—	—
	Total (%) + PET	35 (29.7)	41 (18.8)	NS	28 (40.6)	< 0.001*, 0.019**	—	—	—	—
	Sole total (%)	49 (41.5)	149 (68.3)	< 0.001	—	—	17 (26.2)	—	—	—
	Sole total (%) + PET	7 (14.3)	13 (8.7)	NS	—	—	—	—	—	—

* p value of the positive PET/MRI as compared with sole BME lesions without any other concomitant lesions in the corresponding spinal part. ** p value of the positive PET/MRI as compared with sole FD lesions without any other concomitant lesions in the corresponding spinal part. MRI: magnetic resonance imaging; PET: positron emission tomography (positive finding on PET/MRI indicated by focal 18F-F uptake); SIJ: sacroiliac joints; BME: bone marrow edema; FD: fat deposition; 18F-F: 18F-labeled fluoride; NS: not significant; Total: number of lesions in the corresponding spinal part; Total + PET: number of lesions in the corresponding spinal part in combination with focal 18F-F uptake; Sole total: number of lesions without any other concomitant lesions in the corresponding spinal part; Sole total + PET: number of lesions without any other concomitant lesions in the corresponding spinal part in combination with focal 18F-F uptake.

VQ with all different MRI pathologies. The highest SUVmax was found in VQ, where increased focal 18F-F uptake was associated with the combination of BME and FD (25.7 ± 21.1), followed by VQ where focal 18F-F uptake was associated with FD, but no BME (23.1 ± 18.0), and VQ where focal 18F-F uptake was associated with BME, but not FD (20.7 ± 17.9, all p = not significant). Focal 18F-F uptake without association with any MRI lesions had a mean SUVmax of 21.3 ± 9.5.

DISCUSSION

Integrated PET/MRI has been introduced to clinical practice and is believed to provide a diagnostic tool with high potential for molecular imaging in malignant and inflam-

matory diseases[16,17]. To our knowledge, this current pilot study is the first to examine the use of integrated 18F-F PET/MRI (which is able to depict osteoblastic activity) in patients with an inflammatory rheumatic disease. We found that the integrated acquisition of 18F-F PET and MRI produces high-quality PET as well as MR data and PET/MRI fusion images (Figure 1D, Figure 2D, Figure 3D) with precise spatial coregistration. The integrated scanning approach overcomes the disadvantages of patient re-bedding with potential problems in spatial coregistration that the few available studies on this topic using sequential acquired PET/CT and additional MRI may have had[11,12].

Using these techniques, we found that in patients with active AS, the most frequent MRI lesion associated with osteoblastic activity is BME. In our study, > 70% of the joints examined in the SQ and > 10% in the VQ showed such an association. In contrast, FD alone was associated with osteoblastic activity only in a minority of the examined quadrants (< 9% in both the SIJ and the spine). Nevertheless, when combined with BME, the proportion of quadrants with FD and association with focal 18F-F uptake increased to > 70% in the SIJ and to > 40% in the spine. These data suggest that osteoblastic activity, and subsequently new bone formation, which is the hallmark of imaging findings in AS for both the SIJ and the spine, could be directly linked. Further, even for the SpA-related FD, which is believed to represent postinflammatory lesions, osteoblastic activity only seems to play a role if BME is present in parallel. Finally, in the SIJ, other pathologic lesions such as erosions, sclerosis, or bone bridges as signs of ankylosis were not associated with increased osteoblastic activity. These findings are in line with our previously published data where we could show that for the future development of syndesmophytes, which represent the longterm result of osteoblastic activity, a direct link to BME is needed[6]. Further, these data support the finding that the parallel occurrence of inflammation and subsequent FD on MRI is significantly associated with syndesmophyte formation on conventional radiographs after a followup of 5 years[8]. On the other hand, these data bring into question the role of chronic SIJ changes such as FD or erosions regarding their value to predict future bone formation and ankylosis in the absence of parallel BME, despite their value as diagnostic signs of axSpA[18,19].

In addition to these findings, the SUVmax in 18F-F PET showed a similar pattern, with SUVmax mean values being higher in quadrants that combined BME and FD, as compared with quadrants with FD only or BME only. Nevertheless, these differences were only numerical, suggesting that osteoblastic activity, when present, is not different among the concomitant MRI lesions and that the differences in prevalence of focal 18F-F uptake with other concomitant lesions on MRI is not based on the vitality of the underlying bone tissue, but on its relationship to osteoblastic activity in general.

Our findings are in contrast to the results of 2 earlier studies that used 18F-F PET/CT and sequentially acquired MRI. Those studies found that increased tracer uptake was only modestly correlated to BME on MRI and was more frequently correlated to structural rather than to inflammatory changes[11,12]. These previous studies used the occurrence of syndesmophytes on CT as the gold standard of evaluation, while PET was not integrated with MRI, to collect information on the fluoride uptake to either BME or FD using the hybrid technique that we used. Further, in our study, we did not use CT, and therefore direct comparisons are not possible. Nevertheless, the data presented herein are clinically more relevant than the already published data because, by examining BME and FD on MRI, we were able to depict osteoblastic activity in areas that are affected by the disease even before the final stage of the development of new bone formation, such as syndesmophyte formation, which would have been the case if we had used CT. The question of whether 18F-F PET/MRI depicts earliest disease-related changes of the bone metabolism in axSpA even before MR signal pathologies occur cannot be answered at the current stage. However, we found a substantial number of lesions with isolated 18F-F uptake without simultaneous MR signal pathology in both the spine and SIJ. This isolated tracer uptake could also be nonspecific, e.g., attributable to degenerative changes. However, because of the underlying pathomechanism of axSpA lesions, the relevance of isolated 18F-F uptake, as well as any combination of 18F-F uptake with other lesions, is of potential predictive value for osteoproliferation and should be further analyzed in prospective studies with followup data.

The observation that more lesions were found positive in the SIJ than in the spine by both inflammatory or osteoblastic activity are in line with the clinical observation that the disease-related pathology in established AS is driven by the involvement of the SIJ, while spinal involvement occurs in even later stages of the disease[20]. This is different from what we know from patients with nonradiographic axSpA, where patients with normal MR images of the SIJ might still show increased inflammatory activity in the spinal MRI[21]. Thus, despite the low number of patients, our data seem indeed to represent the findings expected from daily practice when dealing with AS-related imaging findings.

The main limitation of the present study is the small number of the examined patients, which requires the statistical analyses to be interpreted with caution. Because of the small sample size, we were not able to adjust our analysis for multiple comparison and dependency problems. We decided to undertake an exploratory analysis on the basis of single lesions, which is also an approach reflecting daily practice, when evaluating images of either the SIJ or the spine in AS. Another limitation is the low specificity of positive lesions that can be found on PET/MRI, which can be caused by nonspecific tracer uptake in sites of degenerative changes and

can lead to false-positive findings. However, because the 2 readers who interpreted the images in our study are very experienced in the interpretation of MRI lesions related to AS, and because the gold standard used in our study was the lesions found on MRI and not on PET/MRI, the misinterpretation of lesions has not played a significant role in our results. PET attenuation correction in hybrid PET/MRI is challenging, and because the default algorithm of the vendor that was used for our study does not perfectly correct for bone, this might potentially have led to an underestimation of bone tracer uptake in our study. Longitudinal data are required to confirm the findings of this pilot study, especially to prove the direct link between inflammatory MRI pathologies, increased osteoblastic activity depicted by 18F-F PET, and subsequent syndesmophyte formation.

In this pilot study with hybrid 18F-F PET-MRI in patients with active AS, we were able to show that BME rather than chronic changes are associated with osteoblastic activity. Hybrid 18F-F PET-MRI can potentially visualize the sites of the axial skeleton with bone metabolism and BME, post-inflammatory FD, and possibly also future regions of new bone formation in both the spine and SIJ in AS. Further, FD is also important in this process, but almost only in combination with BME. This seems to be similar in both the SIJ and the spine. Whether treating patients earlier, even before the stage of AS has occurred, can lead to a complete inhibition of osteoblastic activity and new bone formation remains to be shown.

REFERENCES

1. Braun J, Sieper J. Ankylosing spondylitis. Lancet 2007;369:1379-90.
2. van der Heijde D, Sieper J, Maksymowych WP, Dougados M, Burgos-Vargas R, Landewé R, et al; Assessment of SpondyloArthritis international Society. 2010 Update of the international ASAS recommendations for the use of anti-TNF agents in patients with axial spondyloarthritis. Ann Rheum Dis 2011;70:905-8.
3. Braun J, van den Berg R, Baraliakos X, Boehm H, Burgos-Vargas R, Collantes-Estevez E, et al. 2010 update of the ASAS/EULAR recommendations for the management of ankylosing spondylitis. Ann Rheum Dis 2011;70:896-904.
4. Rudwaleit M, Listing J, Brandt J, Braun J, Sieper J. Prediction of a major clinical response (BASDAI 50) to tumour necrosis factor alpha blockers in ankylosing spondylitis. Ann Rheum Dis 2004;63:665-70.
5. Baraliakos X, Listing J, Rudwaleit M, Haibel H, Brandt J, Sieper J, et al. Progression of radiographic damage in patients with ankylosing spondylitis: defining the central role of syndesmophytes. Ann Rheum Dis 2007;66:910-5.
6. Baraliakos X, Listing J, Rudwaleit M, Sieper J, Braun J. The relationship between inflammation and new bone formation in patients with ankylosing spondylitis. Arthritis Res Ther 2008;10:R104.
7. Baraliakos X, Listing J, Fritz C, Haibel H, Alten R, Burmester GR, et al. Persistent clinical efficacy and safety of infliximab in ankylosing spondylitis after 8 years—early clinical response predicts long-term outcome. Rheumatology 2011;50:1690-9.
8. Baraliakos X, Heldmann F, Callhoff J, Listing J, Appelboom T, Brandt J, et al. Which spinal lesions are associated with new bone formation in patients with ankylosing spondylitis treated with anti-TNF agents? A long-term observational study using MRI and conventional radiography. Ann Rheum Dis 2014;73:1819-25.
9. Buchbender C, Sewerin P, Mattes-György K, Miese F, Wittsack HJ, Specker C, et al. Utility of combined high-resolution bone SPECT and MRI for the identification of rheumatoid arthritis patients with high-risk for erosive progression. Eur J Radiol 2013;82:374-9.
10. Hawkins RA, Choi Y, Huang SC, Hoh CK, Dahlbom M, Schiepers C, et al. Evaluation of the skeletal kinetics of fluorine-18-fluoride ion with PET. J Nucl Med 1992;33:633-42.
11. Fischer DR, Pfirrmann CW, Zubler V, Stumpe KD, Seifert B, Strobel K, et al. High bone turnover assessed by 18F-fluoride PET/CT in the spine and sacroiliac joints of patients with ankylosing spondylitis: comparison with inflammatory lesions detected by whole body MRI. EJNMMI Res 2012;2:38.
12. Bruijnen ST, van der Weijden MA, Klein JP, Hoekstra OS, Boellaard R, van Denderen JC, et al. Bone formation rather than inflammation reflects ankylosing spondylitis activity on PET-CT: a pilot study. Arthritis Res Ther 2012;14:R71.
13. van der Linden S, Valkenburg HA, Cats A. Evaluation of diagnostic criteria for ankylosing spondylitis. A proposal for modification of the New York criteria. Arthritis Rheum 1984;27:361-8.
14. Garrett S, Jenkinson T, Kennedy LG, Whitelock H, Gaisford P, Calin A. A new approach to defining disease status in ankylosing spondylitis: the Bath Ankylosing Spondylitis Disease Activity Index. J Rheumatol 1994;21:2286-91.
15. Baraliakos X, Listing J, von der Recke A, Braun J. The natural course of radiographic progression in ankylosing spondylitis—evidence for major individual variations in a large proportion of patients. J Rheumatol 2009;36:997-1002.
16. Buchbender C, Heusner TA, Lauenstein TC, Bockisch A, Antoch G. Oncologic PET/MRI, part 1: tumors of the brain, head and neck, chest, abdomen, and pelvis. J Nucl Med 2012;53:928-38.
17. Buchbender C, Schneider M, Ostendorf B. [Magnetic resonance tomography and hybrid imaging in rheumatology]. [Article in German] Z Rheumatol 2013;72:137-44.
18. Weber U, Lambert RG, Pedersen SJ, Hodler J, Ostergaard M, Maksymowych WP. Assessment of structural lesions in sacroiliac joints enhances diagnostic utility of magnetic resonance imaging in early spondylarthritis. Arthritis Care Res 2010;62:1763-71.
19. Wick MC, Weiss RJ, Jaschke W, Klauser AS. Erosions are the most relevant magnetic resonance imaging features in quantification of sacroiliac joints in ankylosing spondylitis. J Rheumatol 2010;37:622-7.
20. Sieper J, Rudwaleit M, Baraliakos X, Brandt J, Braun J, Burgos-Vargas R, et al. The Assessment of SpondyloArthritis international Society (ASAS) handbook: a guide to assess spondyloarthritis. Ann Rheum Dis 2009;68 Suppl 2:ii1-44.
21. van der Heijde D, Sieper J, Maksymowych WP, Brown MA, Lambert RG, Rathmann SS, et al. Spinal inflammation in the absence of sacroiliac joint inflammation on magnetic resonance imaging in patients with active nonradiographic axial spondyloarthritis. Arthritis Rheumatol 2014;66:667-73.